J|A|C|S COMMUNICATIONS

Published on Web 07/27/2010

Magic Angle Spinning NMR Investigation of Influenza A $M2_{18-60}$: Support for an Allosteric Mechanism of Inhibition

Loren B. Andreas,[†] Matthew T. Eddy,[†] Rafal M. Pielak,[‡] James Chou,[‡] and Robert G. Griffin*,[†]

Francis Bitter Magnet Laboratory and Department of Chemistry, Massachusetts Institute of Technology, Cambridge, Massachusetts 02139, and Department of Biological Chemistry and Molecular Pharmacology, Harvard Medical School, Boston, Massachusetts 02115

Received February 22, 2010; E-mail: rgg@mit.edu

Abstract: The tetrameric M2 proton channel from influenza A virus conducts protons at low pH and is inhibited by aminoadamantyl drugs such as amantadine and rimantadine (Rmt). We report magic angle spinning NMR spectra of POPC and DPhPC membrane-embedded $M2_{18-60}$, both apo and in the presence of Rmt. Similar line widths in the spectra of apo and bound M2 indicate that Rmt does not have a significant impact on the dynamics or conformational heterogeneity of this construct. Substantial chemical shift changes for many residues in the transmembrane region support an allosteric mechanism of inhibition. An Rmt titration supports a binding stoichiometry of >1 Rmt molecule per channel and shows that nonspecific binding or changes in membrane composition are unlikely sources of the chemical shift changes. In addition, doubling of spectral lines in all of the observed samples provides evidence that the channel assembles with twofold symmetry.

The M2 protein from influenza A virus is a single-pass membrane protein that assembles as a tetramer to form a H^+-selective channel that functions at low pH and is critical in the viral lifecycle. A class of aminoadamantyl inhibitors has become ineffective against many influenza strains because of mutations in the N-terminal region of the channel,[1] thus stimulating great interest in identification of the pharmacologically relevant binding site and the mechanism of inhibition and drug resistance. Discussion of an external, lipid-facing site and a pore-blocking site is ongoing.[2−8] A solution NMR structure[7] in DHPC micelles of $M2_{18-60}$ showed an external binding site at D44 via direct NOE measurements; however, the pharmacological relevance of this binding pocket has been questioned because of possible detergent effects, such as hydrophobic mismatch, which may impact the structure, dynamics, and binding affinity.[4] Pioneering solid-state NMR experiments by Kovacs and Cross[9] using a shorter TM construct, $M2_{22-46}$, in lipid environments[3,10] were followed by diffraction studies in detergent.[8] Some of these results and more recent NMR experiments[3] suggest S31 as a binding site. Recently, an elegant $^{13}C-^{2}H$ REDOR experiment using ^{2}H-labeled drug and ^{13}C-labeled peptide on $M2_{22-46}$ in lipids detected inhibitor near S31 and, at higher drug concentrations, near D44.[4] However, $M2_{22-46}$ exhibits reduced function and drastically reduced inhibition by drug in comparison with $M2_{18-60}$.[6] Furthermore, the similar construct $M2_{21-61}$ has conduction indistinguishable from that of the full length protein.[5] It is presently unclear whether the discrepancy between the two observed binding sites arises due to detergent effects, the highly truncated construct, or other factors. We therefore initiated investigations of the fully functional construct $M2_{18-60}$ in lipid bilayers using magic angle spinning (MAS) NMR spectroscopy. Our chemical shift data reveal global conformational changes upon drug binding that suggest an allosteric mechanism of inhibition as well as peak doubling that indicates a twofold-symmetric tetramer. In addition, a Rmt titration shows the appearance of drug-bound resonances and the disappearance of apo resonances. The effect is saturated at >1 drug per channel.

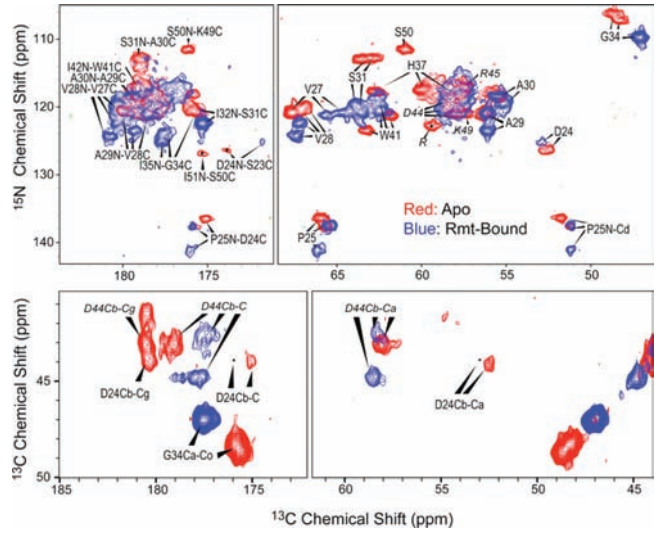

Figure 1. (top) $^{15}N-^{13}C$ zf-TEDOR spectra (τ_{mix} = 1.3 ms) showing assignments of $^{13}C,^{15}N[^{12}C,^{14}N$-ILFY]$M2_{18-60}$ in the drug-bound (blue) and unbound (red) states. Unless otherwise indicated, cross-peaks arise from one-bond N−Cα magnetization transfer. (bottom) $^{13}C-^{13}C$ PDSD spectra (τ_{mix} = 50 ms) showing Asp and Gly cross-peaks of these samples. Sizable chemical shift changes are observed in the N and/or Cα sites for residues 25, 27, 28, 31, 34, 35, 37, and 41. Many peaks are doubled (see Figure S1 in the Supporting Information for an expanded view), notably P25 and A29, supporting the existence of a twofold-symmetric tetramer. Spectra were recorded at pH 7.8 and ∼0 °C. Labels shown in italics (e.g., *D44*) indicate less certainty in the assignments (see the Supporting Information).

The top panel of Figure 1 shows an $^{15}N-^{13}C$ one-bond zf-TEDOR[11,12] correlation spectrum of $M2_{18-60}$ in 1-palmitoyl-2-oleoyl-*sn*-glycero-3-phosphocholine (POPC) bilayers that demonstrates spectral assignments in both the absence (red) and presence (blue) of the inhibitor rimantadine (Rmt). Spectra were recorded with a sample pH of 7.8 and a temperature of 0 °C, just above the phase transition of pure lipid. Line widths of ∼1 ppm for both ^{15}N and ^{13}C were observed at 700 MHz for both drug-bound and apo samples, indicating conformational homogeneity. This narrow line width also indicates that the dynamics of this system are favorable for investigation by MAS NMR spectroscopy. The similarity of the line widths in the bound and apo states is in contrast to the results for $M2_{22-46}$, where drug binding significantly narrowed the spectra,[3] and the improvement using $M2_{18-60}$ could be attributed

[†] Massachusetts Institute of Technology.
[‡] Harvard Medical School.

 10.1021/ja101537p

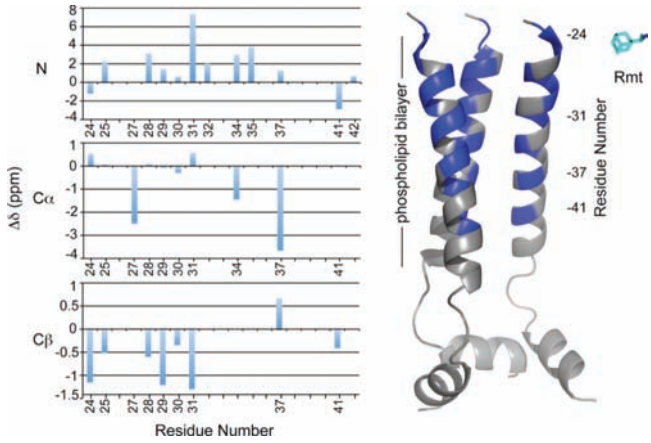

Figure 2. Chemical shift perturbations ($\Delta\delta = \delta_{bound} - \delta_{apo}$) are distributed across the channel and support an allosteric effect upon drug binding. (left) Chemical shift perturbations as a function of residue number. (right) Comparison of the Rmt drug size with the transmembrane tetramer assembly from the solution structure. Blue residues indicate a shift of >2 ppm in N and/or >1 ppm in Cα/Cβ. One of the four helices has been removed for clarity.

to the larger construct, which remains tetrameric even in a sodium dodecyl sulfate detergent environment.[6]

Upon Rmt binding, we observed substantial (>1 ppm ^{13}Cα/Cβ, >2 ppm ^{15}N) chemical shift changes from residues 24 to 41 distributed across the entire range of unambiguously assigned residues and nearly spanning the transmembrane (TM) helix. Significant perturbations occurred for pore-lining residues 27, 34, 37, and 41 and from residues 24, 25, 28, 29, 31, 32, and 35, which are found in the helix−helix interface and lipid-facing sites.[7] Only two of the assigned residues, 30 and 42, showed no chemical shift perturbations of >1 ppm in ^{13}Cα/Cβ or >2 ppm in ^{15}N. In Figure 2, these chemical shift perturbations are shown as a function of residue number and demonstrate significant changes on a length scale many times larger than the ∼5 Å Rmt drug, indicating allostery. We note that the ∼7 ppm shift change at S31 that was observed for M2$_{22-46}$ using amantadine (Amt)[3] was also observed here for M2$_{18-60}$ using Rmt. In addition, we also observed a ∼3.5 ppm shift in H37 Cα, which is comparable considering the ∼2-fold increase in chemical shift variability of ^{15}N relative to ^{13}Cα. Thus, the chemical shift data support an allosteric effect but do not locate the drug; therefore, these data are consistent with the proposed sites of pharmacological relevance, S31 and D44.

An allosteric effect is also in agreement with previous measurements on aligned samples that detected a kink at G34 in Amt-bound M2$_{22-46}$ and a modified conformation upon drug binding.[13] A backbone structure of Amt-bound M2 was calculated in that previous study; however, broad apo spectra compromised a complete structural analysis of that state. From the present spectra, it is clear that the allosteric changes extend across the entire TM domain.

This conclusion relies on the significance of the chemical shift differences between the bound and apo states. Chemical shift changes can arise from several factors, which include changes in secondary structure but can also include variations in solvent, temperature, and pH. Comparisons of chemical shifts for solution and microcrystalline preparations of the same model proteins showed strong agreement (∼1 ppm or less for ^{13}C′ and ^{13}Cα and ∼2 ppm or less for ^{15}N) in the protein core, with somewhat larger differences observed for sites forming crystal contacts in the solid-state preparations.[14−17] The temperature and pH were constant for all of the data reported herein, and the possibility of nonspecific binding and membrane changes are addressed below and in Figures 3 and 4; we have therefore excluded these potential sources of chemical shift perturbations.

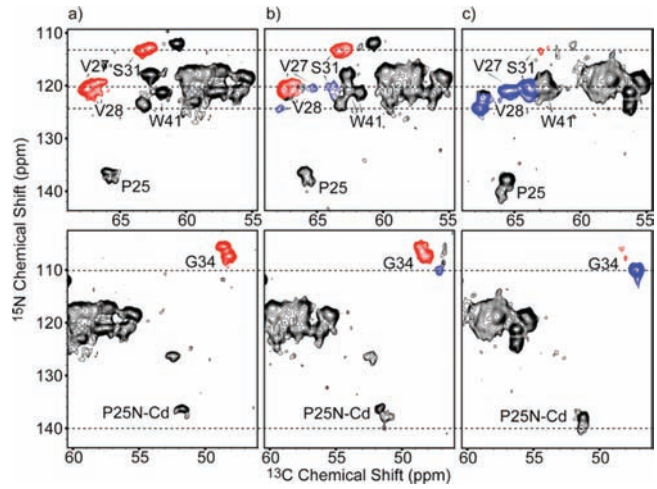

Figure 3. TEDOR spectra acquired at (a) 0, (b) 1, and (c) 4 Rmt molecules per channel result in cross-peaks due to M2 bound to Rmt and present at ∼0, ∼25, and >90%, respectively. The apo spectrum is simultaneously observed at ∼100, ∼75, and <10% of the total site-specific signal intensity. Unless otherwise indicated, cross-peaks arise from one-bond N−Cα magnetization transfer. Resonances that clearly show the titration are displayed in red (unbound form) and blue (Rmt-bound resonances). Dashed lines at G34 and other resonances serve as guides. The signal-to-noise ratio was ∼10 for strong signals. M2 samples used in the titration were embedded in DPhPC lipids and showed spectra nearly identical to those recorded in POPC lipids (see Figure 4**)**. The sample pH was 7.8 and the temperature ∼0 °C.

The solution NMR structure showed an external binding site with a specific interaction between the amine group of Rmt and D44 Cγ. Therefore, we also examined the Asp region of the ^{13}C−^{13}C proton-driven spin diffusion[18] (PDSD) spectra shown in the bottom panel of Figure 1 for perturbations. The G34 Cα−C′ peak exhibited a well-resolved movement upon drug binding and intense peaks in both states, suggesting that it is in a position in the peptide that is not influenced by dynamics. In contrast, the Asp Cβ−C′ and Cβ−Cγ peaks showed reduced intensity that is likely due to motion interfering with cross-polarization (CP) and decoupling.[19,20] Addition of Rmt caused a 2-fold further decrease in these peak intensities and chemical shift changes of several parts per million. A direct H bond between the drug amine and an Asp Cγ carboxyl can explain these effects. However, these effects can also be explained by a large-scale reorganization of the channel resulting in altered conformation and dynamics in the vicinity of the Asp residues.

The zf-TEDOR spectra shown in Figure 3 were acquired at 0, 1, and 4 Rmt molecules per channel in order to investigate binding stoichimetry and rule out the possibility of nonspecific binding. Figure 3a shows an apo spectrum. Upon addition of one Rmt molecule per channel (Figure 3b), resonances of the Rmt-bound form appeared with ∼25% of the total intensity. At four Rmt molecules per channel (Figure 3c), resonances arising from Rmt-bound M2 were primarily observed, with apo resonances still detected at <10% of the total intensity. No gradual change in chemical shifts was observed; rather, the resonances of the bound form appeared in concert, and their intensity increased with increasing Rmt. At 16 Rmt molecules per channel, the effect was saturated, and only the bound form was observed (Figure 1, blue). If these chemical shift changes are due to specific binding, then the resonance intensities suggest a binding stoichiometry of >1 molecule per channel. Notably, pore-facing residues such as G34 and V27, which are unlikely to be affected by any nonspecific hydrophobic interactions or changes in lipid composition, clearly demonstrated the changes. Furthermore, although Rmt is partitioned strongly into the membrane,[21] at one drug molecule per channel it occupied only

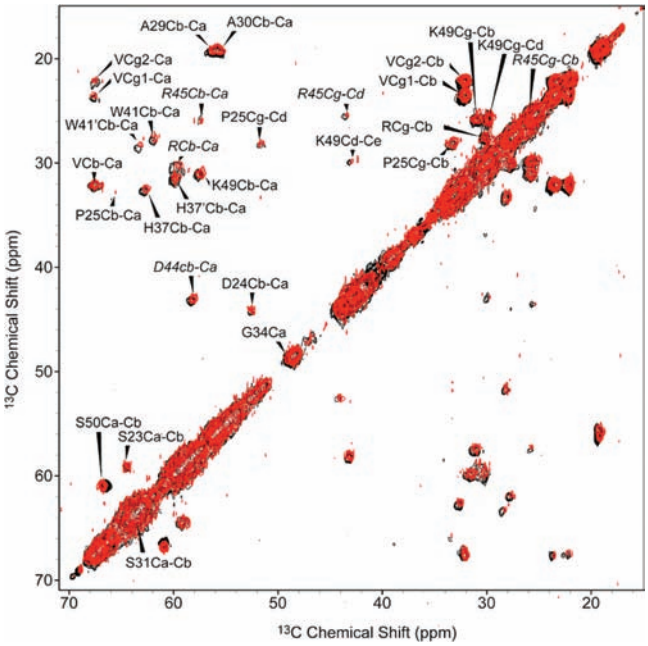

Figure 4. $^{13}C-^{13}C$ PDSD spectra ($\tau_{mix} = 15$ ms) of POPC-embedded (red) and DPhPC-embedded (black) M2 are nearly identical, with maximum chemical shift differences of 0.3 ppm. Mostly one-bond correlations were observed with 15 ms of mixing.

2 mol % of the *nonprotein* membrane components. Neither protein nor M2 tetramer was present in excess, yet all of the chemical shift perturbations were observed. Therefore, if we assume that the pharmacological binding site has high affinity, then nonspecific binding and changes in membrane composition are excluded. The sample pH was 7.8 and the temperature ~0 °C.

Sensitivity to membrane composition was further investigated by collecting TEDOR and PDSD spectra in another lipid, 1,2-diphytanoyl-*sn*-glycero-3-phosphocholine (DPhPC). The spectra recorded in DPhPC are remarkably similar to those of POPC-embedded M2, with maximum chemical shift differences of 0.3 and 0.7 ppm for ^{13}C and ^{15}N, respectively. The PDSD spectra recorded in these two lipids are overlaid in Figure 4. The fact that this change in membrane composition causes small changes in the spectra provides further evidence that the drug-induced chemical shift changes are caused by a specific drug interaction and not by alteration of the membrane composition. Clearly, the state of this construct of M2 in lipids is stable with respect to the change in membrane composition from DPhPC to POPC.

Two distinct sets of peaks with approximately equal intensities were observed for many residues in both apo and drug-bound $M2_{18-60}$, providing evidence that the tetramer is twofold-symmetric. These are most obvious in the P25 cross-peaks in the top panel of Figure 1 but are also apparent in more crowded regions of the spectra. Multiple peak sets could indicate the presence of multiple conformations or arise from incomplete drug binding. However, the peak doubling appears with equal intensities for the two sets of peaks and is found in *both* the apo and drug-bound states, suggesting that the tetrameric assembly has twofold symmetry, which may arise from the packing of the bulky W41 and H37 side chains. This is in agreement with previous work showing that the doubly protonated state of M2 contains two imidazole−imidazolium dimers of H37 and is therefore twofold-symmetric at this position.[22] It is also qualitatively consistent with the diffraction structure at neutral pH, which shows conformational heterogeneity in the C-terminal region.[8] Other structural studies have assumed fourfold symmetry. For example, a single set of resonances was observed for this construct in DHPC micelles[7] and may be the result of fast interconversion between two states at higher temperatures. Also, peak doubling may be present but within the line width observed in previous MAS NMR studies.

Dimerization of two tetramer channels could also lead to two sets of resonances having different chemical shifts at the interface. However, some of the largest separations in doubled peaks appear at residues inside the channel, such as H37 and W41. We therefore find that the most likely explanation for the peak doubling is a twofold-symmetric channel.

In summary, large drug-induced chemical shift changes observed across the entire TM region support a large-scale reorganization of the channel by an allosteric mechanism. In addition, the peak doubling is likely due to twofold symmetry of the tetramer, and the drug titration data are consistent with a binding stoichiometry of >1 Rmt molecule per channel. Determination of the inhibitor binding site on the basis of maximal chemical shift perturbation alone is not possible given the magnitude and distribution of chemical shift changes. Therefore, a direct dipolar coupling measurement[4] between the drug and M2 is needed in order to determine the binding location(s) and thereby elucidate the mechanism of inhibition in a construct such as $M2_{18-60}$ that retains full function in conductance assays.

Acknowledgment. We thank Marcelo Berardi, Alexander Barnes, Christopher Turner, and Eric Miller for helpful discussions. This work was supported by the National Institutes of Health (EB001960, EB002026, and Al067438). L.B.A. was supported by a National Science Foundation Graduate Research Fellowship.

Supporting Information Available: Sample preparation and synthesis, description of assignments, and additional spectra. This material is available free of charge via the Internet at http://pubs.acs.org.

References

(1) Bright, R. A.; Shay, D. K.; Shu, B.; Cox, N. J.; Klimov, A. I. *J. Am. Med. Assoc.* **2006**, *295*, 891–894.
(2) Pielak, R. M.; Chou, J. J. *Protein Cell* **2010**, *1*, 246–258.
(3) Cady, S. D.; Luo, W.; Hu, F.; Hong, M. *Biochemistry* **2009**, *48*, 7356–7364.
(4) Cady, S. D.; Schmidt-Rohr, K.; Wang, J.; Soto, C. S.; DeGrado, W. F.; Hong, M. *Nature* **2010**, *463*, 689–692.
(5) Ma, C.; Polishchuk, A. L.; Ohigashi, Y.; Stouffer, A. L.; Schon, A.; Magavern, E.; Jing, X.; Lear, J. D.; Freire, E.; Lamb, R. A.; DeGrado, W. F.; Pinto, L. H. *Proc. Natl. Acad. Sci. U.S.A.* **2009**, *106*, 12283–12288.
(6) Pielak, R. M.; Schnell, J. R.; Chou, J. J. *Proc. Natl. Acad. Sci. U.S.A.* **2009**, *106*, 7379–7384.
(7) Schnell, J. R.; Chou, J. J. *Nature* **2008**, *451*, 591–595.
(8) Stouffer, A. L.; Acharya, R.; Salom, D.; Levine, A. S.; Di Costanzo, L.; Soto, C. S.; Tereshko, V.; Nanda, V.; Stayrook, S.; DeGrado, W. F. *Nature* **2008**, *451*, 596–599.
(9) Kovacs, F. A.; Cross, T. A. *Biophys. J.* **1997**, *73*, 2511–2517.
(10) Wang, J.; Kim, S.; Kovacs, F.; Cross, T. A. *Protein Sci.* **2001**, *10*, 2241–2250.
(11) Jaroniec, C. P.; Filip, C.; Griffin, R. G. *J. Am. Chem. Soc.* **2002**, *124*, 10728–10742.
(12) Hing, A. W.; Vega, S.; Schaefer, J. *J. Magn. Reson.* **1992**, *96*, 205–209.
(13) Hu, J.; Asbury, T.; Achuthan, S.; Li, C.; Bertram, R.; Quine, J. R.; Fu, R.; Cross, T. A. *Biophys. J.* **2007**, *92*, 4335–4343.
(14) Franks, W. T.; Zhou, D. H.; Wylie, B. J.; Money, B. G.; Graesser, D. T.; Frericks, H. L.; Sahota, G.; Rienstra, C. M. *J. Am. Chem. Soc.* **2005**, *127*, 12291–12305.
(15) Igumenova, T. I.; Wand, A. J.; McDermott, A. E. *J. Am. Chem. Soc.* **2004**, *126*, 5323–5331.
(16) Seidel, K.; Etzkorn, M.; Heise, H.; Becker, S.; Baldus, M. *ChemBioChem* **2005**, *6*, 1638–1647.
(17) van Rossum, B. J.; Castellani, F.; Pauli, J.; Rehbein, K.; Hollander, J.; de Groot, H. J.; Oschkinat, H. *J. Biomol. NMR* **2003**, *25*, 217–223.
(18) Szeverenyi, N. M.; Sullivan, D.; Maciel, G. E. *J. Magn. Reson.* **1982**, *47*, 462–475.
(19) Long, J. R.; Sun, B. Q.; Griffin, R. G. *J. Am. Chem. Soc.* **1994**, *116*, 11950–11956.
(20) Maus, D. G.; Copie, V.; Sun, B. Q.; Griffiths, J. M.; Griffin, R. G.; Luo, S.; Schrock, R. R.; Liu, A. H.; Seidel, S. W.; Davis, W. M.; Grohmann, A. *J. Am. Chem. Soc.* **1996**, *118*, 5665–5671.
(21) Wang, J.; Schnell, J. R.; Chou, J. J. *Biochem. Biophys. Res. Commun.* **2004**, *324*, 212–217.
(22) Hu, J.; Fu, R.; Nishimura, K.; Zhang, L.; Zhou, H. X.; Busath, D. D.; Vijayvergiya, V.; Cross, T. A. *Proc. Natl. Acad. Sci. U.S.A.* **2006**, *103*, 6865–6870. Hu, J.; Fu, R.; Cross, T. A. *Biophys. J.* **2007**, *93*, 276–283.

JA101537P